# Regional Lung Derecruitment and Inflammation during 16 Hours of Mechanical Ventilation in Supine Healthy Sheep

Mauro R. Tucci, M.D., Ph.D.,* Eduardo L. V. Costa, M.D., Ph.D.,† Tyler J. Wellman, M.S.,‡ Guido Musch, M.D.,§ Tilo Winkler, Ph.D.,§ R. Scott Harris, M.D.,|| Jose G. Venegas, Ph.D.,§ Marcelo B. P. Amato, M.D., Ph.D.,# Marcos F. Vidal Melo, M.D., Ph.D.§



## ABSTRACT

**Background:** Lung derecruitment is common during general anesthesia. Mechanical ventilation with physiological tidal volumes could magnify derecruitment, and produce lung dysfunction and inflammation. The authors used positron emission tomography to study the process of derecruitment in normal lungs ventilated for 16 h and the corresponding changes in regional lung perfusion and inflammation.

**Methods:** Six anesthetized supine sheep were ventilated with $V_T$ = 8 ml/kg and positive end-expiratory pressure = 0. Transmission scans were performed at 2-h intervals to assess regional aeration. Emission scans were acquired at baseline and after 16 h for the following tracers: (1) $^{18}$F-fluorodeoxyglucose to evaluate lung inflammation and (2) $^{13}$NN to calculate regional perfusion and shunt fraction.

**Results:** Gas fraction decreased from baseline to 16 h in dorsal (0.31 ± 0.13 to 0.14 ± 0.12, $P < 0.01$), but not in ventral regions (0.61 ± 0.03 to 0.63 ± 0.07, $P$ = nonsignificant), with time constants of 1.5–44.6 h. Although the vertical distribution of relative perfusion did not change from baseline to 16 h, shunt increased in dorsal regions (0.34 ± 0.23 to 0.63 ± 0.35, $P < 0.01$). The average pulmonary net $^{18}$F-fluorodeoxyglucose uptake rate in six regions of interest along the ventral–dorsal direction increased from 3.4 ± 1.4 at baseline to 4.1 ± 1.5 · $10^{-3}$/min after 16 h ($P < 0.01$), and the corresponding average regions of interest $^{18}$F-fluorodeoxyglucose phosphorylation rate increased from 2.0 ± 0.2 to 2.5 ± 0.2 · $10^{-2}$/min ($P < 0.01$).

**Conclusions:** When normal lungs are mechanically ventilated without positive end-expiratory pressure, loss of aeration occurs continuously for several hours and is

### What We Already Know about This Topic

- In normal lungs, induction of anesthesia and muscle paralysis produce lung derecruitment associated with functional deterioration and potentially lung injury and pulmonary infection
- Dynamics of regional lung derecruitment and its relationship to regional perfusion and inflammation remains poorly understood

### What This Article Tells Us That Is New

- In normal sheep lungs mechanically ventilated (over 16 h, 8 ml/kg, zero positive end-expiratory pressure), progressive derecruitment is associated with increased regional shunt, implying insufficient hypoxic pulmonary vasoconstriction, and incipient inflammation

* Research Fellow, Department of Anesthesia, Critical Care and Pain Medicine, Massachusetts General Hospital and Harvard Medical School, Boston, Massachusetts, and Staff Intensivist and Instructor, Respiratory Intensive Care Unit, University of Sao Paulo School of Medicine, São Paulo, Brazil. † Research Fellow, Department of Anesthesia, Critical Care and Pain Medicine, Massachusetts General Hospital and Harvard Medical School; Staff Intensivist and Instructor, Respiratory Intensive Care Unit, University of Sao Paulo School of Medicine; and Assistant Professor, Research and Education Institute, Hospital Síirio-Libanês, Sao Paulo, Brazil. ‡ Ph.D. Student, Department of Biomedical Engineering, Boston University, Boston, Massachusetts. § Associate Professor, Department of Anesthesia, Critical Care and Pain Medicine, Massachusetts General Hospital and Harvard Medical School. || Assistant Professor, Department of Medicine (Pulmonary and Critical Care), Massachusetts General Hospital and Harvard Medical School. # Associate Professor, Respiratory Intensive Care Unit, University of Sao Paulo School of Medicine.

Received from the Department of Anesthesia, Critical Care and Pain Medicine, Massachusetts General Hospital, Boston, Massachusetts. Submitted for publication June 11, 2012. Accepted for publication February 11, 2013. Supported by grant HL 5R01HL086827 from the National Institutes of Health, Bethesda, Maryland. Dr. Tucci received a scholarship from the Coordination for the Improvement of Higher Level Personnel, Brasilia, Brazil. Dr. Musch was supported by grant R01HL094639 from the National Institutes of Health. Presented at the Annual Meeting of the American Society of Anesthesiologists, New Orleans, Louisiana, October 17–21, 2009; abstract number A1379.

Address correspondence to Dr. Vidal Melo: Department of Anesthesia, Critical Care and Pain Medicine, Massachusetts General Hospital, 55 Fruit St., Boston, Massachusetts 02114. mvidalmelo@partners.org. Information on purchasing reprints may be found at www.anesthesiology.org or on the masthead page at the beginning of this issue. ANESTHESIOLOGY's articles are made freely accessible to all readers, for personal use only, 6 months from the cover date of the issue.

 Anesthesiology 2013; 119:156-65

preferentially localized to dorsal regions. Progressive lung derecruitment was associated with increased regional shunt, implying an insufficient hypoxic pulmonary vasoconstriction. The increased pulmonary net uptake and phosphorylation rates of $^{18}$F-fluorodeoxyglucose suggest an incipient inflammation in these initially normal lungs.

IN normal lungs, induction of anesthesia and muscle paralysis produce lung derecruitment with significant atelectasis.[1] These are associated with functional deterioration such as decreased lung compliance, impairment of oxygenation, increased pulmonary vascular resistance, and potentially, the development of lung injury and pulmonary infections.[2,3]

It is generally accepted that derecruitment develops within minutes after induction of general anesthesia with muscular relaxation.[1] However, it is unclear whether and how fast derecruitment progresses after establishment of mechanical ventilation in normal lungs. Indeed, Cai *et al.*[4] reported no change in nonaerated regions up to 7 h after mechanical ventilation with pure oxygen and zero positive end-expiratory pressure (PEEP) in patients with healthy lungs. In contrast, others reported a progressive increase in nonaerated lung after 40–90 min of mechanical ventilation with or without pure oxygen and zero PEEP in patients with normal lungs undergoing neuro or general surgery.[3,5,6]

There is increasing awareness about the risks of lung injury associated with high tidal volumes, and physiological tidal volumes (6–8 ml/kg) have been proposed for mechanical ventilation in the operating room and intensive care unit.[7–9] This practice, however, raises the concern that lung derecruitment could be further facilitated, inducing hypoxemia and inflammation, especially in the absence of an associated PEEP.[2,10] Indeed, experimental studies suggested that mechanical ventilation of the normal lung with low tidal volumes and zero PEEP could lead to stress-related damage to endothelial and alveolar epithelial cells.[11] Consequently, it is important to determine whether lung derecruitment is a progressive process leading to activation of potentially injurious mechanisms in normal lungs ventilated with physiological tidal volumes. As time is a key variable in determining the magnitude of lung injury resulting from mechanical ventilation,[12] that process could be particularly relevant during periods corresponding to long surgeries.

Accordingly, we used multitracer positron emission tomography (PET) imaging to investigate progressive derecruitment during prolonged (16 h) mechanical ventilation by quantifying regional lung aeration and the corresponding changes in $^{18}$F-fluorodeoxyglucose ($^{18}$F-FDG) uptake, a measure of inflammatory cell metabolic activation.[13–15] We also measured regional perfusion because its topographical distribution could be affected by the development of atelectasis and also modulate the development of regional inflammation.[13] Better understanding of the dynamics of regional lung derecruitment and its relation to regional perfusion and inflammation could help to optimize the application of strategies such as PEEP and recruitment maneuvers aimed at minimizing lung injury and maximizing gas exchange during mechanical ventilation of normal lungs. In current study, we ventilated sheep for 16 h with $V_T$ = 8 ml/kg and zero PEEP to reflect the use of physiological tidal volumes and the practice of ventilating anesthetized patients without PEEP, which remains prevalent.[16,17]

## Materials and Methods

All animal experiments were performed in compliance with institutional guidelines approved by the Subcommittee on Research Animal Care at the Massachusetts General Hospital and in accordance with the "Guide for the Care and Use of Laboratory Animals" published by the National Institutes of Health (publ. no. 86-23, revised 1996).

### Experimental Protocol

Six sheep, weighing 22.6 ± 2.4 kg and aged 3–4 months, were anesthetized, intubated, and mechanically ventilated (Ohmeda 7800 ventilator; Datex-Ohmeda, Madison, WI). Anesthesia was maintained with a continuous infusion of ketamine and propofol titrated to heart rate and blood pressure. Paralysis was established with a bolus of pancuronium (0.1 mg/kg) at induction and repeated every 90 min (0.02–0.04 mg/kg). For monitoring and collection of blood samples, we cannulated one femoral artery and introduced a pulmonary artery catheter *via* the right external jugular vein.

The animals were placed supine in the PET scanner (Scanditronix PC4096; General Electric, Milwaukee, WI) with the caudal end of the field of view just superior to the dome of the diaphragm. Final positioning was determined after a recruitment maneuver with airway pressure held at 40 cm $H_2O$ for 30 s. Sheep were mechanically ventilated for 16 h with a volume control mode, $V_T$, 8 ml/kg; PEEP, 0; inspired oxygen fraction ($F_{IO_2}$), ≥0.3 (adjusted to maintain an arterial oxygen saturation ≥90% measured by cooximetry [OSM3; Radiometer, Copenhagen, Denmark]), inspiratory-to-expiratory ratio, 1:2, initial respiratory rate of 18 breaths/min, and adjusted to maintain the arterial carbon dioxide partial pressure ($Pa_{CO_2}$) between 32 and 45 mmHg. Physiological data were collected at baseline and at 4-h intervals. At the end of the study, the animals were euthanized with intravenous administration of bolus injection of potassium chloride.

### PET Imaging Protocol and Processing

The experimental system and methods of analysis have been previously presented in detail.[15,18–20] The PET camera collected 15 transverse slices of 6.5-mm thickness providing three-dimensional information over a 9.7-cm–long field of view, which we previously estimated to encompass approximately 70% of the total sheep lung volume. Resulting images consisted of an interpolated matrix of 128 × 128 × 15 voxels with a size of 2.0 × 2.0 × 6.5 mm$^3$ each. Three different types of PET images were acquired:

1. **Transmission scans**: using a rotating pin-source of $^{68}$Ge for 10 min[20] were obtained at baseline and 2-h intervals, resulting in nine scans for each animal. From these, the following variables were calculated:
   a. Gas fraction ($F_{gas}$)[20]: calculated for the whole lung and for six coronal regions of interest (ROIs) of equal heights along the ventral–dorsal axis (ROI 1 was the most ventral and ROI 6 the most dorsal) for all nine scans. The squared coefficient of variation ($CV^2$ = [SD/mean])$^2$ was used to quantify the voxel-by-voxel heterogeneity of $F_{gas}$ in the whole imaged lung.[21]
   b. Relative nonaerated lung volume defined as the percentage of the total lung volume with $F_{gas}$ less than 0.1.[22] $Nonaerated_{volume}$ was calculated as:[23]

$$\text{Nonaerated}_{\text{volume}} = \frac{\text{Number nonaerated voxels}}{\text{Total number of voxels}} \times 100$$

   c. Relative nonaerated lung mass as a percentage of total lung mass ($Nonaerated_{mass}$) was calculated as the sum of the densities ($D = 1 - F_{gas}$) of all nonaerated voxels divided by the sum of the densities of all voxels within the field of view:[23]

$$\text{Nonaerated}_{\text{mass}} = \frac{\sum_{\text{i=1, non aerated voxels}} D_i}{\sum_{\text{i =1, all voxels}} D_i} \times 100$$

   d. Regional time constant for regional loss of aeration: to quantify the rate of regional derecruitment, regional $F_{gas}$ was fitted with an exponential function:

$$F_{gas}(t) = F_{gas}(\text{baseline}) \cdot e^{-t/\tau} + F_{gas}(\text{end})$$

where $F_{gas}(t)$ is the regional measurement at time $t$, $F_{gas}$(baseline) is the $F_{gas}$ value at baseline (after recruitment maneuver), $F_{gas}$(end) is the asymptotic $F_{gas}$ value, and $\tau$ is the time constant of $F_{gas}$ decrease over time (*i.e.*, time required for approximately 63% decrease in $F_{gas}$). Visual inspection of the time course of $F_{gas}$ revealed little temporal variation in coronal ROIs 1–4. We therefore calculated $\tau$ only for ROIs 5 and 6.

2. **Emission scans after intravenous $^{13}$NN-saline**: performed at baseline and at the end of the 16-h mechanical ventilation period. Analysis of the lung tracer kinetics of $^{13}$NN after an intravenous injection of $^{13}$NN-saline during a 60-s apnea at mean lung volume was used to compute voxel level perfusion[20] and allowed for the measurement of the following:
   a. Relative pulmonary perfusion: relative perfusion to each of the six ROIs was computed as the peak regional $^{13}$NN activity (mean of all voxels of the ROI) measured after the $^{13}$NN bolus injection divided by the sum of the peak activities of all ROIs.

   Perfusion heterogeneity: measured on a voxel-by-voxel basis using squared coefficients of variation of perfusion ($CV^2_{\dot{Q}}$) and of density-normalized perfusion ($CV^2_{\dot{Q}/D}$) computed by voxel-by-voxel division of perfusion by the respective density.
   b. Regional pulmonary shunt: shunt in each ROI was derived by modeling the kinetics of $^{13}$NN.[19,24]

3. **Emission scans after intravenous administration of $^{18}$F-FDG**: obtained for quantification of regional $^{18}$F-FDG kinetics. After $^{13}$NN clearance, $^{18}$F-FDG (~5 mCi) was infused at a constant rate through the jugular catheter for 60 s. Starting at the beginning of $^{18}$F-FDG infusion, sequential PET frames (9 × 10 s, 4 × 15 s, 1 × 30 s, 7 × 60 s, 15 × 120 s, 1 × 300 s, and 3 × 600 s) were acquired over 75 min whereas pulmonary arterial blood was sampled at 5.5, 9.5, 25, 37, and 42.5 min.[13] The $^{18}$F-FDG kinetics in each ROI was fitted to a three-compartment model consisting of an intravascular compartment, a precursor compartment representing the concentration of $^{18}$F-FDG available for phosphorylation (*i.e.*, the concentration of $^{18}$F-FDG that can serve as a substrate for hexokinase), and a metabolized compartment accounting for the concentration of $^{18}$F-FDG that has been phosphorylated by hexokinase.[25,26] In this analysis, the $^{18}$F-FDG net uptake rate ($K_i$), a measure of cellular metabolic activity, is expressed as: $K_i = F_e \cdot k_3$; the constant $k_3$ is the rate of $^{18}$F-FDG phosphorylation, proportional to hexokinase activity, and $F_e$ is the fraction of the ROI occupied by the precursor compartment.[25,27] $K_i$, $k_3$, and $F_e$ were calculated for each of the six coronal ROIs.

### Selection of Voxels for Analysis

For each animal, two lung masks were created: one at baseline and another at 16 h. The masks were created using a semiautomatic method. An initial mask was generated by automatic threshold selection combining aerated regions from transmission scans and nonaerated perfused regions from $^{13}$NN perfusion scans. This mask was manually refined to exclude areas corresponding to main bronchi and large pulmonary vessels.

For the analysis of temporal changes in aeration, a single mask was created, which contained voxels present both at baseline and 16 h (*i.e.*, this mask represented the "intersection" of the baseline and 16 h masks).

### Blood and Lung Neutrophil Counts and Histological Examination

After euthanasia, the lungs of four animals were excised and filled with Trump's fixative to a pressure of 25 cm $H_2O$. After fixation, a block of lung tissue was sampled from the ventral and dorsal regions and embedded in paraffin. Sections of

5 μm were cut, mounted, and stained with hematoxylin and eosin for light microscopy. Alveolar and septal neutrophils were counted in 10 randomly selected high-power (×400) fields per slide (1 ventral and 1 dorsal slide per animal) by a reader blinded to the sampled tissue identification. In addition, alveolar edema, alveolar hemorrhage, septal thickening, and capillary congestion were evaluated semiquantitatively with a modified four-grade scale (absent = 0, mild = 1, moderate = 2, and marked = 3).[28] Leukocyte count was measured at the start and end of the protocol in five animals.

### Statistical Analysis

Variables were tested for normality with the Shapiro–Wilk test. Data are expressed as median and interquartile ranges (IQR 25, 75%) or as mean ± SD. We compared physiological values before and after 16 h of mechanical ventilation with paired Student *t* test when data were normally distributed or with Wilcoxon signed-rank test when data were not normally distributed. PET-acquired data ($F_{gas}$, perfusion, shunt, and $^{18}$F-FDG variables) were compared at two time points (baseline and 16 h) and among the six ROIs with a linear mixed-effect model. The categorical variables time and ROI and their interaction (when significant) were modeled as fixed effects, and the variation among individuals for each variable was modeled with random coefficients for the intercepts. Bonferroni *post hoc* tests were performed when the overall *P* values were less than 0.05. Multivariate regression for the six animals at the nine time points was used to study the dependence of relative nonaerated lung mass on $F_{IO_2}$ and time points. Analyses were performed using SPSS version 13 (SPSS, Chicago, IL). All statistical tests were two-tailed, and significance was set at *P* less than 0.05.

## Results

### Physiologic Variables at Baseline and after 16 Hours of Mechanical Ventilation

Peak airway pressure increased, whereas dynamic compliance, $Pa_{O_2}/F_{IO_2}$ ratio, and pH decreased from baseline to 16 h (table 1). Respiratory rate, $Pa_{CO_2}$, and cardiovascular variables were stable in the same period (table 1).

### Regional Lung Aeration

At baseline, there was a heterogeneous vertical distribution of $F_{gas}$ ($P < 0.001$; fig. 1). Mean $F_{gas}$ in ventral ROIs were within the normal range ($0.5 < F_{gas} < 0.9$), whereas dorsal ROIs (ROIs 5–6) had mean $F_{gas}$ less than 0.5, compatible with poor aeration. There was a significant change in the regional distribution of $F_{gas}$ after 16 h of mechanical ventilation ($P < 0.01$). Although ventral regions (ROIs 1–2) presented minimal changes in $F_{gas}$ over time ($0.61 \pm 0.03$ *vs.* $0.63 \pm 0.07$, *P* = nonsignificant), dorsal regions (ROIs 5–6) showed significant reduction of $F_{gas}$ ($0.31 \pm 0.13$ *vs.* $0.14 \pm 0.12$, $P < 0.01$; figs. 1 and 2). The decrease in $F_{gas}$ with time in ROIs 5 and 6 had time constants of 24.0 h (IQR 14.9–35.7 h) and 10.7 h (IQR 4.3–11.3 h), respectively (fig. 3). There was a significant increase in spatial heterogeneity of $F_{gas}$ ($CV^2_{Fgas}$) from baseline to 16 h (table 2).

In line with the changes in $F_{gas}$, nonaerated lung volume increased after 16 h (0.8% IQR 0.2–3.5 to 12.6% IQR 11.2–17.8; $P = 0.03$; fig. 4A), as did nonaerated lung mass (1.5 IQR 0.3–5.8% to 19.2 IQR 18.1–26.1%; $P = 0.03$, fig. 4B). In five of the six animals, nonaerated lung comprised more than 3% of the lung volume throughout the protocol (fig. 4). Multivariate regression showed a significant dependence of nonaerated lung mass on $F_{IO_2}$ ($P < 0.05$).

**Table 1.** Global Physiological Variables at Baseline and 16 Hours

| | Baseline | 16 h |
|---|---|---|
| Mean arterial pressure, mmHg | 95 ± 4 | 88 ± 13 |
| Mean pulmonary arterial pressure, mmHg | 11 ± 5 | 14 ± 7 |
| Cardiac output, l/min | 5.4 ± 1.1 | 4.7 ± 0.9 |
| Heart rate, beats/min | 154 ± 24 | 143 ± 39 |
| $Pv_{O_2}$, mmHg | 39 ± 3 | 46 ± 6 |
| Tidal volume, ml | 204 ± 28 | 198 ± 19 |
| Tidal volume, ml/kg | 9.0 ± 1.1 | 8.8 ± 0.7 |
| Respiratory rate, breaths/min | 26 ± 3 | 24 ± 3 |
| Peak airway pressure, cm $H_2O$ | 16.8 ± 5.7 | 26.0 ± 7.6* |
| Dynamic compliance, ml/cm $H_2O$ | 12.5 ± 3.2 | 7.82 ± 2.0* |
| pH | 7.43 ± 0.05 | 7.32 ± 0.10* |
| $Pa_{O_2}$, mmHg | 86 ± 34 | 66 ± 11 |
| $Pa_{CO_2}$, mmHg | 33 ± 4.4 | 35 ± 2.3 |
| $F_{IO_2}$ | 0.30 (0.30–0.35) | 0.50 (0.30–0.60) |
| $Pa_{O_2}/F_{IO_2}$, mmHg | 274 ± 129 | 152 ± 67* |
| Blood neutrophil count, 1/μl | 2,094 ± 628 | 4,721 ± 1481* |

* $P < 0.05$ for the comparison with baseline; values are mean ± SD or median (interquartile range).

$F_{IO_2}$ = inspired fraction of oxygen; $Pa_{CO_2}$ = arterial partial pressure of carbon dioxide; $Pa_{O_2}/F_{IO_2}$ = ratio between arterial partial pressure of oxygen and $F_{IO_2}$; $Pv_{O_2}$ = mixed venous partial pressure of oxygen.

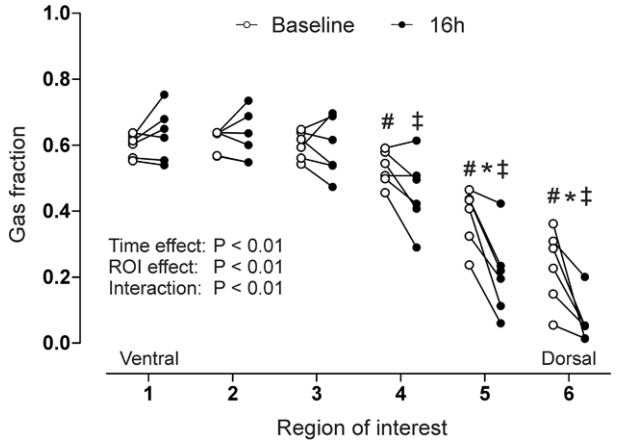


**Fig. 1.** Mean regional gas fraction ($F_{gas}$) for all animals (n = 6) at baseline and after 16 h of mechanical ventilation in six coronal regions of interest (ROIs) of equal height along the ventral–dorsal axis (ROI 1 is the most ventral and ROI 6 the most dorsal). Note that a significant decrease in gas fraction occurred only in dorsal regions (ROIs 5–6). *$P$ < 0.05 (baseline *vs.* 16 h); #$P$ < 0.01 (*vs.* previous ROI at baseline); ‡$P$ < 0.05 (*vs.* previous ROI at 16 h).

### Regional Lung Perfusion and Regional Shunt

At baseline and after 16 h of mechanical ventilation, relative perfusion was lowest in most of the ventral regions and increased progressively along the ventral–dorsal axis to reach a plateau at ROIs 4–6 (fig. 5). Relative perfusion to each ROI was not significantly redistributed after 16 h of mechanical ventilation ($P$ = 0.99, figs. 2C and 5), even though the spatial heterogeneity of perfusion tended to increase over time, irrespective of whether this heterogeneity was calculated with ($P$ = 0.09) or without ($P$ = 0.10) normalization of perfusion by voxel-by-voxel tissue density (table 2).

At baseline, regional shunt fractions were negligible in ventral regions (ROIs 1–2) but increased progressively toward dorsal regions (ROIs 5–6, fig. 6; 0.34 ± 0.23 *vs.* 0.63 ± 0.35, $P$ < 0.01). After 16 h, global shunt fraction was markedly higher than at baseline (table 2) due to a significant increase in shunt in dorsal regions (ROIs 5–6, fig. 6).

### Regional $^{18}$F-FDG Kinetics and Neutrophilic Inflammation

At baseline and after 16 h of mechanical ventilation, $K_i$ had a heterogeneous vertical distribution with dorsal regions (ROIs 5–6, figs. 2D and 7) showing higher values than ventral regions. The regional distribution of the volume of the precursor compartment ($F_e$) paralleled the distribution of $K_i$, whereas $k_3$ was homogeneously distributed along the vertical axis (fig. 7).

After 16 h of mechanical ventilation, $K_i$ was significantly increased ($P$ < 0.01; fig. 7). This increase was homogeneous in all ROIs as reflected by the nonsignificant interaction term (fig. 7) and was related to an increase in $k_3$ ($P$ < 0.01), without change in $F_e$ ($P$ = 0.65; fig 7). Average ROI $K_i$ increased from 3.4 ± 1.4 at baseline to 4.1 ± 1.5 · $10^{-3}$/min after 16 h

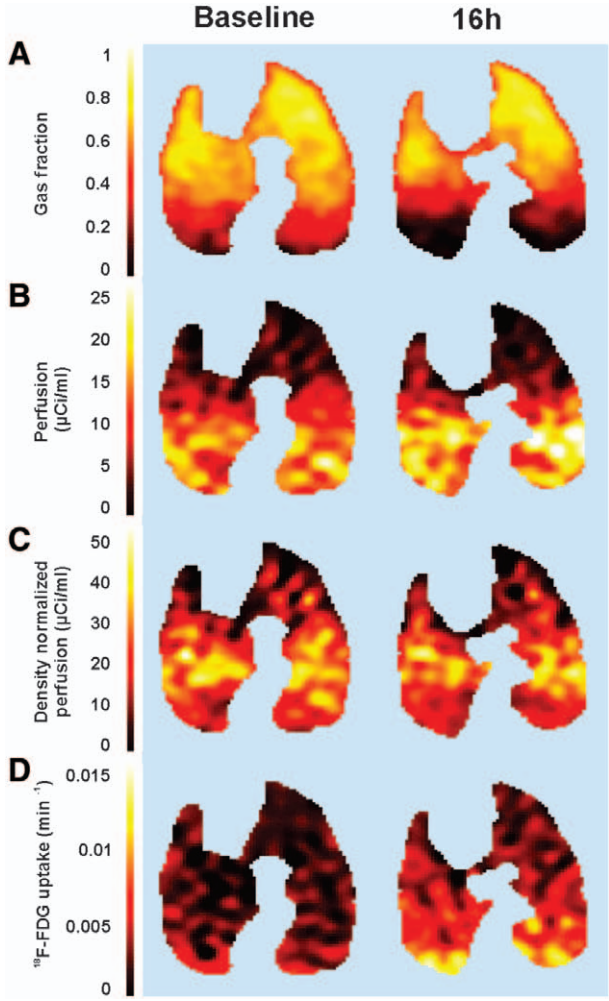


**Fig. 2.** Images of (*A*) lung aeration, (*B*) perfusion, (*C*) density-normalized perfusion, and (*D*) $^{18}$F-fluorodeoxyglucose ($^{18}$F-FDG) net uptake rate at the beginning (baseline) and end of the study (16 h) for a typical case. In this example, there is a decrease in gas fraction in dorsal regions from baseline to 16 h (*A*), associated with an increase in perfusion in the same regions (*B*). After normalization by density (lung tissue; *C*), such increase in perfusion in dorsal regions was no longer visualized. $^{18}$F-FDG uptake (*D*) increased from baseline to 16 h.

($P$ < 0.01), and the corresponding average ROI $k_3$ increased from 2.0 ± 0.2 to 2.5 ± 0.2 · $10^{-2}$/min ($P$ < 0.01).

### Histology

Blood neutrophil counts more than doubled from baseline to the end of 16 h of mechanical ventilation (table 1). Lung neutrophil counts were low and not significantly different between ventral (4.2 neutrophils/field IQR 2.8–6.7) and dorsal regions (6.7 IQR 5.3–7.6) at the end of the protocol. Histological analysis revealed mild septal edema and capillary congestion in dorsal regions in a predominantly normal parenchyma with no alveolar edema or hemorrhage.

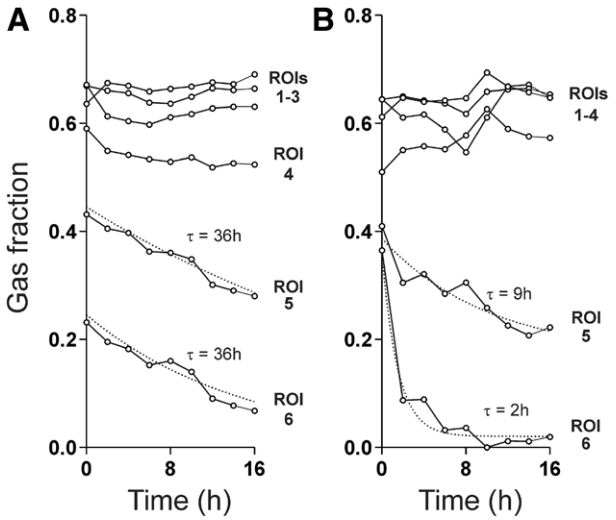


**Fig. 3.** Time course of gas fraction ($F_{gas}$) in six coronal regions of interest (ROIs) of equal height along the ventral–dorsal axis (ROI 1 is the most ventral and ROI 6 the most dorsal) during 16 h of mechanical ventilation for two animals with different time constants of dorsal lung derecruitment. Temporal changes in $F_{gas}$ were not significant in nondependent regions. In contrast, dorsal regions (ROIs 5 and 6) showed systematic loss of aeration, with variability in time constants (τ): (*A*) case of equal and long time constants in ROI 5 and 6. (*B*) Case with different and shorter time constants for the same ROIs. The *dotted lines* indicate the exponential fitting.

## Discussion

The main findings of this study of prolonged mechanical ventilation with physiological tidal volumes and zero PEEP in supine healthy sheep were the following: (1) loss of lung aeration with corresponding increase in volume and mass of nonaerated lung occurred progressively along 16 h of mechanical ventilation. Time constants suggested the continuation of lung derecruitment beyond that period in some animals; (2) the spatial distribution of the loss of aeration was heterogeneous, with dorsal regions accounting for most of the aeration loss; (3) shunt in dorsal regions increased with time whereas regional relative perfusion did not change after 16 h despite ongoing atelectasis in dorsal regions. Thus, hypoxic pulmonary vasoconstriction was not effective enough to avoid the increase in shunt and deterioration of gas exchange; and (4) there was an increase in the net $^{18}$F-FDG uptake at 16 h, predominantly due to increase in the rate constant $k_3$, which describes $^{18}$F-FDG phosphorylation. Despite this increase, regional net $^{18}$F-FDG uptake values at 16 h were still within a range compatible with values measured in normal lung regions.[13,15,29]

The chosen $V_T$ was consistent with current recommendations for normal lungs.[10] We used PEEP = 0 because use of no or minimal PEEP still represents a prevalent practice in the operating room,[16,17] even though such approaches differ from current recommendations.[10]

We observed marked topographical heterogeneity in the process of aeration loss. Atelectasis during anesthesia is commonly understood to be caused by a fall in functional residual capacity, associated airway closure, and reabsorption atelectasis.[3,5,30] Anesthetized mechanically ventilated patients with normal lungs present a vertical gradient in lung aeration produced by the gradient in local transpulmonary pressures.[31] However, it is unknown how this aeration gradient changes over long periods of mechanical ventilation. We showed progressive dorsal lung derecruitment, contrasting with no change in ventral aeration over 16 h. If those aeration gradients were to depend exclusively on vertical position, they would not be expected to change with time. Thus, our results indicate that time-dependent factors play a key role in determining the vertical distribution of aeration in normal lungs.

There are conflicting data on temporal changes in lung derecruitment after initiation of mechanical ventilation. Although some studies reported no additional derecruitment once aeration loss was established,[1,4,32] others indicated progressive derecruitment.[3,5,6] Our measurements revealed large time constants for dorsal derecruitment (1.5–44.6 h), a finding that contrasts with previous results suggesting rapid stabilization.[1,33] The observed increased peak airway pressure and decreased dynamic compliance and $Pa_{O_2}/F_{I_{O_2}}$ from baseline to 16 h reinforce the functional relevance of that progressive derecruitment. Previous results were mostly based

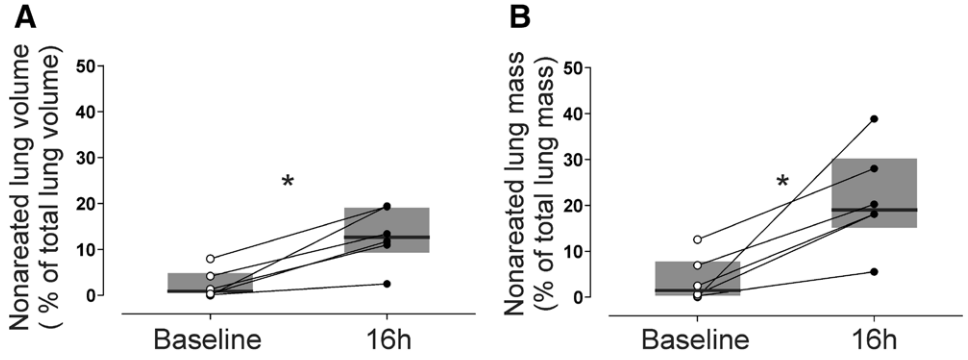


**Fig. 4.** Amount of nonaerated lung (gas fraction <0.1) for all animals (n = 6) at baseline and at 16 h shown as percentage of lung volume (*A*) and percentage of lung tissue mass (*B*). Median (*solid line*) and interquartile range (*gray box*) are represented.

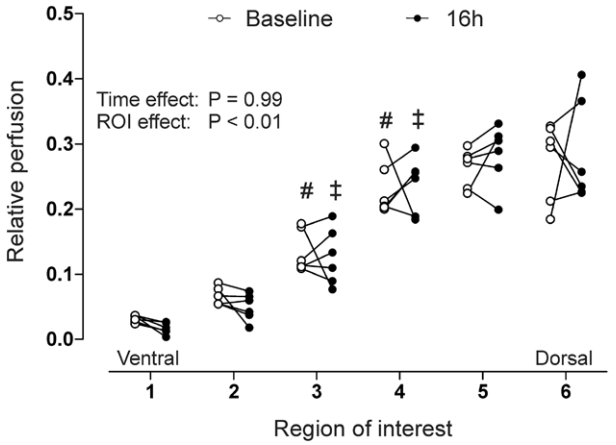


**Fig. 5.** Regional relative perfusion *versus* six coronal regions of interest (ROIs) of equal heights along the ventral–dorsal axis (ROI 1 is the most ventral and ROI 6 the most dorsal) at baseline and after 16 h of mechanical ventilation presented for all animals (n = 6). #$P < 0.01$ (*vs.* previous ROI at baseline); ‡$P < 0.05$ (*vs.* previous ROI at 16 h).

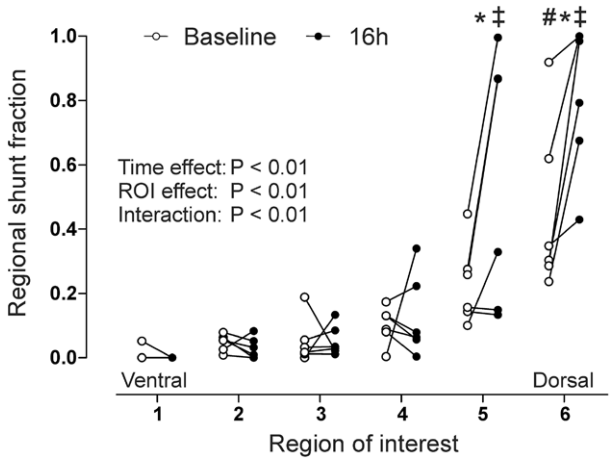


**Fig. 6.** Regional shunt fraction at baseline and after 16 h for the six coronal regions of interest (ROIs) along the ventral–dorsal axis measured in all animals (n = 6; ROI 1 is the most ventral and ROI 6 the most dorsal). *$P < 0.05$ (baseline *vs.* 16 h); #$P < 0.01$ (*vs.* previous ROI at baseline); ‡$P < 0.05$ (*vs.* previous ROI at 16 h).

on short periods (14–20 min).[1,33] A study on supine neurosurgical patients did not show significant derecruitment after 7 h.[4] The differences between our findings and those of the aforementioned studies may result from the longer periods of observation in our study. Our findings concur with the progressive loss of aeration observed in patients after 40–90 min of mechanical ventilation with PEEP = 0.[3,5,6] The measured derecruitment time constants further indicate that derecruitment may continue for hours to days. This knowledge is of clinical importance because it shows that progressive lung derecruitment, rather than deterioration of the lung condition, may explain day-to-day decreases in oxygenation or changes in radiographic presentation.

At least three mechanisms could explain the observed regional lung derecruitment: compression atelectasis,[2] absorption atelectasis,[2] and airway–parenchymal interdependence.[34,35] Although compression atelectasis would explain the initial loss of aeration, it cannot entirely account for the results as it develops within minutes.[36,37] The fact that we found an association between $F_{IO_2}$ and amount of nonaerated tissue is consistent with a contribution of absorption atelectasis to derecruitment. However, given the study design, derecruitment could have prompted the increases in $F_{IO_2}$ to maintain the target oxygen saturation. Our measured derecruitment time constants are consistent with theoretical time constants during gas absorption due to complete or partial airway closure.[30,38] Finally, airway–parenchymal interdependence could be an additional contributing factor as parenchymal tethering is reduced at low lung volumes,[34,35] resulting in airway closure and lung derecruitment. Muscle relaxants[39] and propofol,[40] used in this study, reduce functional residual capacity by facilitating some of the discussed mechanisms.

**Table 2.** Imaging Derived Variables at Baseline and 16 Hours

| Variable | Baseline | 16 h |
|---|---|---|
| Aeration | | |
| $F_{gas}$ | 0.51 (0.44, 0.52) | 0.42 (0.37, 0.52) |
| $CV^2_{Fgas}$ | 0.10 ± 0.05 | 0.26 ± 0.10* |
| Perfusion | | |
| $CV^2_{\dot{Q}}$ | 0.34 ± 0.09 | 0.52 ± 0.27 |
| $CV^2_{\dot{Q}/D}$ | 0.28 ± 0.05 | 0.40 ± 0.17 |
| Shunt fraction | 0.13 (0.11, 0.21) | 0.33 (0.14, 0.55)* |

* $P < 0.05$. Values are mean ± SD or median (interquartile range). All variables are dimensionless.

$CV^2_{Fgas}$ = squared coefficient of variation of Fgas; $CV^2_{\dot{Q}}$ = squared coefficient of variation of perfusion; $CV^2_{\dot{Q}/D}$ = squared coefficient of variation of perfusion normalized by density; Fgas = gas fraction.

At baseline, perfusion was distributed predominantly to middle and dorsal lung, even after normalization by tissue density (fig. 2, B and C). After 16 h of mechanical ventilation, we did not observe a significant redistribution of perfusion, despite the loss of aeration in dorsal regions, even though spatial heterogeneity of perfusion tended to increase (table 2). Such results suggest a trend to increase nongravitational heterogeneity of perfusion. They also contradict the expectation that perfusion would substantially decrease in regions of reduced aeration due to intact hypoxic pulmonary vasoconstriction in the normal lung.[41] Instead, we found increased regional shunt in dorsal regions (fig. 6) and deterioration in global gas exchange (increased global shunt, table 2). This finding confirms that dorsal regions contribute significantly to gas exchange dysfunction and that hypoxic pulmonary vasoconstriction was insufficient to avoid the increase in shunt.

Several factors could explain the absence of perfusion redistribution in the vertical direction: (1) overdistension

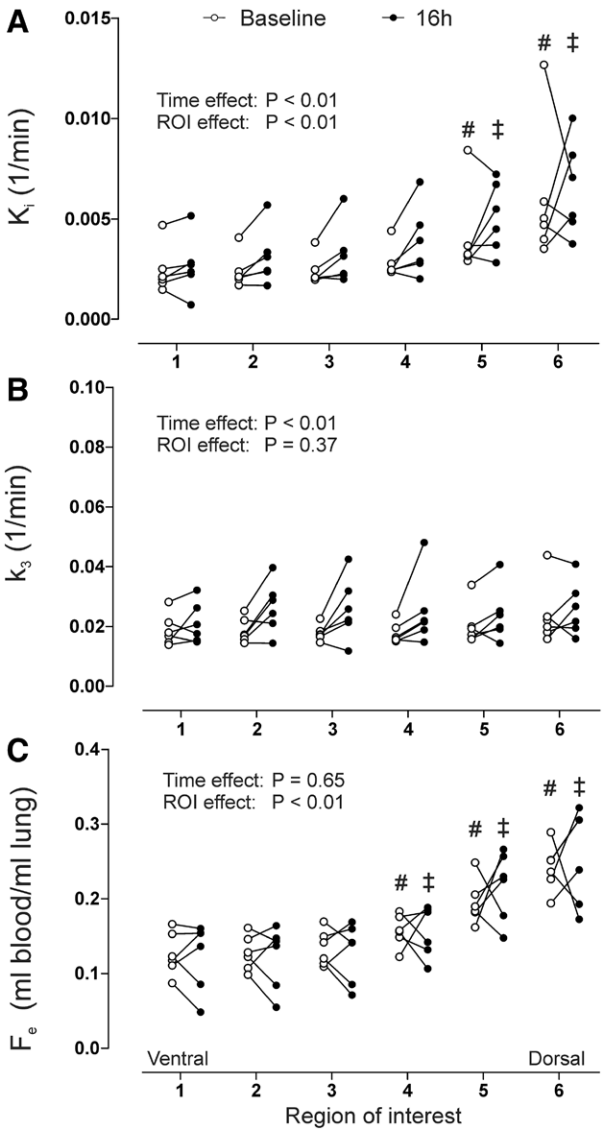


**Fig. 7.** Regional net $^{18}$F-fluorodeoxyglucose ($^{18}$F-FDG) uptake rate. (*A*) Regional net $^{18}$F-fluorodeoxyglucose uptake rate (Ki), (*B*) rate of $^{18}$F-FDG trapping, proportional to hexokinase activity (k3), and (*C*) fraction of lung volume occupied by the extravascular substrate compartment (Fe) at baseline and after 16 h for all animals (n = 6) in six coronal regions of interest (ROIs) of equal height along the ventral–dorsal axis (ROI 1 is the most ventral and ROI 6 the most dorsal). #$P < 0.01$ (*vs.* previous ROI at baseline); ‡$P < 0.05$ (*vs.* previous ROI at 16 h).

of the aerated lung diverting blood flow to nonaerated regions,[18,42] resulting from a fixed $V_T$ applied in the presence of substantial nonaerated lung; (2) inhibition of hypoxic pulmonary vasoconstriction due to early inflammation;[43] and (3) attenuation of hypoxic pulmonary vasoconstriction by high mixed venous oxygen tension.[44] Further investigation will be required to determine those mechanisms.

$K_i$ and $k_3$ were significantly increased after 16 h of mechanical ventilation, compatible with neutrophil activation in the early stages of lung injury.[13–15] Increases in $K_i$[15] and $k_3$ (representing the $^{18}$F-FDG rate of phosphorylation)[45] have been used to measure increases in cell activity and inflammation. Thus, they could be indicative of a preinjury condition. The changes in $k_3$, suggestive of increased metabolic activity per cell, explain most of the changes in $K_i$. The absence of histological signs of significant damage, compatible with the absence of temporal changes in $F_e$, reinforces the interpretation that the increases in $K_i$ and $k_3$ are possible early events in the pathogenesis of ventilator-induced lung injury, suggestive of a mild and incipient inflammatory process. Indeed, such incipient inflammation is likely reversible[46] but could progress if the lungs are ventilated for longer periods of time[9] or in the presence of a second injurious stimulus.[13]

Values of $K_i$ both at baseline and after 16 h of mechanical ventilation were within the range found previously in control lungs of healthy sheep.[13,15,29] Consequently, they conflict with previous estimates of concentration of stress in derecruited normal lung.[47] The absence of a regionalized increase in $k_3$ could suggest that the increase in $K_i$ after 16 h was either not associated to injurious factors—ventral hyperinflation and dorsal low-volume injury—or that these factors resulted in similar consequences to inflammation. Another possibility is that the increase in $^{18}$F-FDG uptake rate represents a broader proinflammatory effect caused by mild cyclical stretching of macrophages and epithelial cells.[48,49] It is tempting to hypothesize that such metabolic changes could be modified by interventions such as PEEP, recruitment maneuvers, and prone position. Indeed, a recent study showed improved lung function and reduced pulmonary infection scores when a protective ventilatory strategy, predominantly based on PEEP = 10 *versus* 0 cm $H_2O$, was used intraoperatively during abdominal surgery.[50] Such findings are compatible with the current study's suggestion of incipient inflammation during ventilation at low lung volumes, even when tidal volumes are not exaggerated, and with the PEEP-induced reduction of lung mechanical injury at all length scales.[51]

Limitations of the imaging techniques have been discussed in detail.[13,15,20,52] The field of view of the PET scanner encompassed approximately 70% of the lung,[20] omitting portions of the apex and base. The large amount of nonareated tissue at 16 h could be explained partially by species differences: we studied young sheep, which are known to have reduced collateral ventilation potentially facilitating reabsorption atelectasis.[53] As peak instead of plateau pressures were measured, changes in airway resistance in addition to alveolar collapse could have contributed to the observed increases in airway pressure. Although no gas humidifier was used during the study, no endotracheal tube obstruction was noticed after inspection at the end of the experiment, suggesting that this was unlikely to have affected the measured peak pressures. Given that all animals received a muscle relaxant, our results may not directly apply to conditions in which muscle relaxants are not used, such as intensive care unit patients. Additionally, factors such as presence of acute respiratory distress syndrome, sepsis, prone position, and

PEEP importantly influence lung derecruitment, and our results cannot be directly extrapolated to those cases.

In summary, lung derecruitment occurred as a continuous process along 16 h in supine sheep with previously healthy lungs mechanically ventilated with physiological tidal volume and zero PEEP. The increase in the amount of nonaerated lung in dorsal regions did not affect the distribution of relative perfusion, and was associated with an increase in regional shunt, indicating an insufficient hypoxic pulmonary vasoconstriction. There was an increase in the net $^{18}$F-FDG uptake at 16 h, associated with an increase in the rate of $^{18}$F-FDG phosphorylation, suggestive of incipient inflammation.

The authors thank Steven B. Weise (Senior Research Technician, Division of Nuclear Medicine, Massachusetts General Hospital, Boston, Massachusetts) for image acquisition and processing; and Peter A. Rice, B.S., R.Ph., and Stephen C. Dragotakes, R.Ph. (Certified Nuclear Pharmacists, Department of Radiology, Massachusetts General Hospital); John A. Correia, Ph.D. (Associate Professor of Radiology, Harvard Medical School, Boston, Massachusetts); William M. Buceliewicz (Senior Cyclotron Engineer, Department of Radiology, Massachusetts General Hospital); and David F. Lee, B.S. (Senior Cyclotron Engineer, Department of Radiology, Massachusetts General Hospital), for preparation of the radioisotopes.

## References

1. Brismar B, Hedenstierna G, Lundquist H, Strandberg A, Svensson L, Tokics L: Pulmonary densities during anesthesia with muscular relaxation—A proposal of atelectasis. Anesthesiology 1985; 62:422–8
2. Duggan M, Kavanagh BP: Pulmonary atelectasis: A pathogenic perioperative entity. Anesthesiology 2005; 102:838–54
3. Rothen HU, Sporre B, Engberg G, Wegenius G, Högman M, Hedenstierna G: Influence of gas composition on recurrence of atelectasis after a reexpansion maneuver during general anesthesia. Anesthesiology 1995; 82:832–42
4. Cai H, Gong H, Zhang L, Wang Y, Tian Y: Effect of low tidal volume ventilation on atelectasis in patients during general anesthesia: A computed tomographic scan. J Clin Anesth 2007; 19:125–9
5. Rothen HU, Sporre B, Engberg G, Wegenius G, Reber A, Hedenstierna G: Prevention of atelectasis during general anaesthesia. Lancet 1995; 345:1387–91
6. Gunnarsson L, Strandberg A, Brismar B, Tokics L, Lundquist H, Hedenstierna G: Atelectasis and gas exchange impairment during enflurane/nitrous oxide anaesthesia. Acta Anaesthesiol Scand 1989; 33:629–37
7. Sundar S, Novack V, Jervis K, Bender SP, Lerner A, Panzica P, Mahmood F, Malhotra A, Talmor D: Influence of low tidal volume ventilation on time to extubation in cardiac surgical patients. Anesthesiology 2011; 114:1102–10
8. Lellouche F, Dionne S, Simard S, Bussières J, Dagenais F: High tidal volumes in mechanically ventilated patients increase organ dysfunction after cardiac surgery. Anesthesiology 2012; 116:1072–82
9. Gajic O, Dara SI, Mendez JL, Adesanya AO, Festic E, Caples SM, Rana R, St Sauver JL, Lymp JF, Afessa B, Hubmayr RD: Ventilator-associated lung injury in patients without acute lung injury at the onset of mechanical ventilation. Crit Care Med 2004; 32:1817–24
10. Schultz MJ, Haitsma JJ, Slutsky AS, Gajic O: What tidal volumes should be used in patients without acute lung injury? Anesthesiology 2007; 106:1226–31
11. D'Angelo E, Pecchiari M, Gentile G: Dependence of lung injury on surface tension during low-volume ventilation in normal open-chest rabbits. J Appl Physiol 2007; 102:174–82
12. Tsuno K, Prato P, Kolobow T: Acute lung injury from mechanical ventilation at moderately high airway pressures. J Appl Physiol 1990; 69:956–61
13. Costa EL, Musch G, Winkler T, Schroeder T, Harris RS, Jones HA, Venegas JG, Vidal Melo MF: Mild endotoxemia during mechanical ventilation produces spatially heterogeneous pulmonary neutrophilic inflammation in sheep. Anesthesiology 2010; 112:658–69
14. Jones HA, Clark RJ, Rhodes CG, Schofield JB, Krausz T, Haslett C: *In vivo* measurement of neutrophil activity in experimental lung inflammation. Am J Respir Crit Care Med 1994; 149:1635–9
15. Musch G, Venegas JG, Bellani G, Winkler T, Schroeder T, Petersen B, Harris RS, Melo MF: Regional gas exchange and cellular metabolic activity in ventilator-induced lung injury. Anesthesiology 2007; 106:723–35
16. Blum JM, Fetterman DM, Park PK, Morris M, Rosenberg AL: A description of intraoperative ventilator management and ventilation strategies in hypoxic patients. Anesth Analg 2010; 110:1616–22
17. Fernández-Pérez ER, Sprung J, Afessa B, Warner DO, Vachon CM, Schroeder DR, Brown DR, Hubmayr RD, Gajic O: Intraoperative ventilator settings and acute lung injury after elective surgery: A nested case control study. Thorax 2009; 64:121–7
18. Musch G, Bellani G, Vidal Melo MF, Harris RS, Winkler T, Schroeder T, Venegas JG: Relation between shunt, aeration, and perfusion in experimental acute lung injury. Am J Respir Crit Care Med 2008; 177:292–300
19. O'Neill K, Venegas JG, Richter T, Harris RS, Layfield JD, Musch G, Winkler T, Melo MF: Modeling kinetics of infused 13NN-saline in acute lung injury. J Appl Physiol 2003; 95:2471–84
20. Vidal Melo MF, Layfield D, Harris RS, O'Neill K, Musch G, Richter T, Winkler T, Fischman AJ, Venegas JG: Quantification of regional ventilation-perfusion ratios with PET. J Nucl Med 2003; 44:1982–91
21. Vidal Melo MF, Winkler T, Harris RS, Musch G, Greene RE, Venegas JG: Spatial heterogeneity of lung perfusion assessed with (13)N PET as a vascular biomarker in chronic obstructive pulmonary disease. J Nucl Med 2010; 51:57–65
22. Gattinoni L, Presenti A, Torresin A, Baglioni S, Rivolta M, Rossi F, Scarani F, Marcolin R, Cappelletti G: Adult respiratory distress syndrome profiles by computed tomography. J Thorac Imaging 1986; 1:25–30
23. Borges JB, Okamoto VN, Matos GF, Caramez MP, Arantes PR, Barros F, Souza CE, Victorino JA, Kacmarek RM, Barbas CS, Carvalho CR, Amato MB: Reversibility of lung collapse and hypoxemia in early acute respiratory distress syndrome. Am J Respir Crit Care Med 2006; 174:268–78
24. Galletti GG, Venegas JG: Tracer kinetic model of regional pulmonary function using positron emission tomography. J Appl Physiol 2002; 93:1104–14
25. Schroeder T, Vidal Melo MF, Musch G, Harris RS, Venegas JG, Winkler T: Modeling pulmonary kinetics of 2-deoxy-2-[18F] fluoro-D-glucose during acute lung injury. Acad Radiol 2008; 15:763–75
26. Sokoloff L, Reivich M, Kennedy C, Des Rosiers MH, Patlak CS, Pettigrew KD, Sakurada O, Shinohara M: The [14C]deoxyglucose method for the measurement of local cerebral glucose utilization: Theory, procedure, and normal values in the conscious and anesthetized albino rat. J Neurochem 1977; 28:897–916
27. de Prost N, Tucci MR, Melo MF: Assessment of lung inflammation with 18F-FDG PET during acute lung injury. AJR Am J Roentgenol 2010; 195:292–300

28. Mikawa K, Maekawa N, Nishina K, Takao Y, Yaku H, Obara H: Effect of lidocaine pretreatment on endotoxin-induced lung injury in rabbits. Anesthesiology 1994; 81:689–99
29. Schroeder T, Vidal Melo MF, Musch G, Harris RS, Winkler T, Venegas JG: PET imaging of regional 18F-FDG uptake and lung function after cigarette smoke inhalation. J Nucl Med 2007; 48:413–9
30. Dantzker DR, Wagner PD, West JB: Instability of lung units with low $V_A/Q$ ratios during $O_2$ breathing. J Appl Physiol 1975; 38:886–95
31. Hachenberg T, Lundquist H, Tokics L, Brismar B, Hedenstierna G: Analysis of lung density by computed tomography before and during general anaesthesia. Acta Anaesthesiol Scand 1993; 37:549–55
32. Strandberg A, Tokics L, Brismar B, Lundquist H, Hedenstierna G: Atelectasis during anaesthesia and in the postoperative period. Acta Anaesthesiol Scand 1986; 30:154–8
33. Edmark L, Kostova-Aherdan K, Enlund M, Hedenstierna G: Optimal oxygen concentration during induction of general anesthesia. Anesthesiology 2003; 98:28–33
34. Venegas JG, Winkler T, Musch G, Vidal Melo MF, Layfield D, Tgavalekos N, Fischman AJ, Callahan RJ, Bellani G, Harris RS: Self-organized patchiness in asthma as a prelude to catastrophic shifts. Nature 2005; 434:777–82
35. Yap DY, Liebkemann WD, Solway J, Gaver DP III: Influences of parenchymal tethering on the reopening of closed pulmonary airways. J Appl Physiol 1994; 76:2095–105
36. Hedenstierna G, Strandberg A, Brismar B, Lundquist H, Svensson L, Tokics L: Functional residual capacity, thoracoabdominal dimensions, and central blood volume during general anesthesia with muscle paralysis and mechanical ventilation. Anesthesiology 1985; 62:247–54
37. Tokics L, Hedenstierna G, Brismar B, Strandberg A, Lundquist H: Thoracoabdominal restriction in supine men: CT and lung function measurements. J Appl Physiol 1988; 64:599–604
38. Joyce CJ, Williams AB: Kinetics of absorption atelectasis during anesthesia: A mathematical model. J Appl Physiol 1999; 86:1116–25
39. Tokics L, Strandberg A, Brismar B, Lundquist H, Hedenstierna G: Computerized tomography of the chest and gas exchange measurements during ketamine anaesthesia. Acta Anaesthesiol Scand 1987; 31:684–92
40. von Ungern-Sternberg BS, Frei FJ, Hammer J, Schibler A, Doerig R, Erb TO: Impact of depth of propofol anaesthesia on functional residual capacity and ventilation distribution in healthy preschool children. Br J Anaesth 2007; 98:503–8
41. Fernandez-Bustamante A, Easley RB, Fuld M, Mulreany D, Hoffman EA, Simon BA: Regional aeration and perfusion distribution in a sheep model of endotoxemic acute lung injury characterized by functional computed tomography imaging. Crit Care Med 2009; 37:2402–11
42. Musch G, Harris RS, Vidal Melo MF, O'Neill KR, Layfield JD, Winkler T, Venegas JG: Mechanism by which a sustained inflation can worsen oxygenation in acute lung injury. Anesthesiology 2004; 100:323–30
43. Caironi P, Ichinose F, Liu R, Jones RC, Bloch KD, Zapol WM: 5-Lipoxygenase deficiency prevents respiratory failure during ventilator-induced lung injury. Am J Respir Crit Care Med 2005; 172:334–43
44. Domino KB, Wetstein L, Glasser SA, Lindgren L, Marshall C, Harken A, Marshall BE: Influence of mixed venous oxygen tension (PVO2) on blood flow to atelectatic lung. Anesthesiology 1983; 59:428–34
45. Okazumi S, Isono K, Enomoto K, Kikuchi T, Ozaki M, Yamamoto H, Hayashi H, Asano T, Ryu M: Evaluation of liver tumors using fluorine-18-fluorodeoxyglucose PET: Characterization of tumor and assessment of effect of treatment. J Nucl Med 1992; 33:333–9
46. Vaneker M, Halbertsma FJ, van Egmond J, Netea MG, Dijkman HB, Snijdelaar DG, Joosten LA, van der Hoeven JG, Scheffer GJ: Mechanical ventilation in healthy mice induces reversible pulmonary and systemic cytokine elevation with preserved alveolar integrity: An *in vivo* model using clinical relevant ventilation settings. Anesthesiology 2007; 107:419–26
47. Mead J, Takishima T, Leith D: Stress distribution in lungs: A model of pulmonary elasticity. J Appl Physiol 1970; 28:596–608
48. Saha D, Takahashi K, de Prost N, Winkler T, Pinilla-Vera M, Baron RM, Vidal Melo MF: Micro-autoradiographic assessment of cell types contributing to 2-deoxy-2-[(18)F]fluoro-D-glucose uptake during ventilator-induced and endotoxemic lung injury. Mol Imaging Biol 2013; 15:19–27
49. Gharib SA, Liles WC, Klaff LS, Altemeier WA: Noninjurious mechanical ventilation activates a proinflammatory transcriptional program in the lung. Physiol Genomics 2009; 37:239–48
50. Severgnini P, Selmo G, Lanza C, Chiesa A, Frigerio A, Bacuzzi A, Dionigi G, Novario R, Gregoretti C, Abreu MG, Schultz MJ, Jaber S, Futier E, Chiaranda M, Pelosi P: Protective mechanical ventilation during general anesthesia for open abdominal surgery improves postoperative pulmonary function. Anesthesiology 2013; 118:1307–21
51. Wellman TJ, Winkler T, Costa EL, Musch G, Harris RS, Venegas JG, Vidal Melo MF: Effect of regional lung inflation on ventilation heterogeneity at different length scales during mechanical ventilation of normal sheep lungs. J Appl Physiol 2012; 113:947–57
52. Wellman TJ, Winkler T, Costa EL, Musch G, Harris RS, Venegas JG, Melo MF: Measurement of regional specific lung volume change using respiratory-gated PET of inhaled 13N-nitrogen. J Nucl Med 2010; 51:646–53
53. Terry PB, Menkes HA, Traystman RJ: Effects of maturation and aging on collateral ventilation in sheep. J Appl Physiol 1987; 62:1028–32